Cellular Microbiology (2015) **17**(10), 1510–1522
doi:10.1111/cmi.12453
First published online 5 June 2015

Atg8 is involved in endosomal and phagosomal acidification in the parasitic protist *Entamoeba histolytica*

Karina Picazarri,[1†] Kumiko Nakada-Tsukui,[1†] Kumiko Tsuboi,[1] Eri Miyamoto,[1,2] Naoko Watanabe,[2] Eiryo Kawakami[1,4] and Tomoyoshi Nozaki[1,3*]
[1]*Department of Parasitology, National Institute of Infectious Diseases, Tokyo, Japan.*
[2]*Department of Biomolecular Science, Faculty of Science, Toho University, Chiba, Japan.*
[3]*Graduate School of Life and Environmental Sciences, University of Tsukuba, Tsukuba, Japan.*
[4]*Laboratory for Disease Systems Modeling, RIKEN Center for integrative Medical Sciences, 1-7-22 Suehiro-cho, Tsurumi-ku, Yokohama, Kanagawa, Japan.*

Summary

Autophagy is one of two major bulk protein degradation systems and is conserved throughout eukaryotes. The protozoan *Entamoeba histolytica*, which is a human intestinal parasite, possesses a restricted set of autophagy-related (Atg) proteins compared with other eukaryotes and thus represents a suitable model organism for studying the minimal essential components and ancestral functions of autophagy. *E. histolytica* possesses two conjugation systems: Atg8 and Atg5/12, although a gene encoding Atg12 is missing in the genome. Atg8 is considered to be the central and authentic marker of autophagosomes, but recent studies have demonstrated that Atg8 is not exclusively involved in autophagy per se, but other fundamental mechanisms of vesicular traffic. To investigate this question in *E. histolytica*, we studied on Atg8 during the proliferative stage. Atg8 was constitutively expressed in both laboratory-maintained and recently established clinical isolates and appeared to be lipid-modified in logarithmic growth phase, suggesting a role of Atg8 in non-stress and proliferative conditions. These findings are in contrast to those for *Entamoeba invadens*, in which autophagy is markedly induced during an early phase of differentiation from the trophozoite into the cyst. The repression of Atg8 gene expression in *En. histolytica* by antisense small RNA-mediated transcriptional gene silencing resulted in growth retardation, delayed endocytosis and reduced acidification of endosomes and phagosomes. Taken together, these results suggest that Atg8 and the Atg8 conjugation pathway have some roles in the biogenesis of endosomes and phagosomes in this primitive eukaryote.

Introduction

Autophagy is widely conserved in eukaryotes and has many physiological functions, including nutrient scavenging, cell development, tumorigenesis, defence against intracellular pathogens, degradation of ubiquitinated protein aggregates and organelle removal (Takeshige *et al.*, 1992; Tsukada and Ohsumi, 1993; Komatsu and Ichimura, 2010; Mehrpour *et al.*, 2010; Wang and Levine, 2010; Mizushima and Komatsu, 2011; Mizushima *et al.*, 2011; Loos *et al.*, 2013). For this reason, the molecular mechanisms of autophagy are being actively studied in a number of model organisms. In free-living and parasitic protists, genetic and functional analyses have revealed that majority of autophagy-related (Atg) proteins are conserved, but some components are occasionally missing or present as multiple copies and may play lineage-specific roles (Brennand *et al.*, 2011; Duszenko *et al.*, 2011). Atg3, 4, 7 and 8, which are involved in one of the two ubiquitin-like conjugation systems, are highly conserved in all eukaryotic 'supergroups' (Keeling *et al.*, 2005) and, Atg8, in particular, is considered to be a reliable marker for autophagosomes as it is localized to isolation membrane and remains associated with autophagosomes during a course of authophagosome maturation (Kabeya *et al.*, 2000).

Starvation-induced autophagy was demonstrated in a number of protists including *Tetrahymena*, *Trypanosoma cruzi*, *Trypanosoma brucei*, *Leishmania major*, *Toxoplasma gondii*, *Plasmodium falciparum* and *Trichomonas vaginalis* (Nilsson, 1984; Kaneda *et al.*, 1991; Benchimol,

Received 7 August, 2014; revised 9 April, 2015; accepted 23 April, 2015. *For correspondence. E-mail nozaki@nih.go.jp; Tel. (+81) 3 4580 2690; Fax: (+81) 3 5285 1173.
†These authors equally contributed to this work.

1999; Alvarez *et al*., 2008; Williams *et al*., 2009; Besteiro *et al*., 2011; Li *et al*., 2012; Tomlins *et al*., 2013). It has also been shown that autophagy plays a role in differentiation in *L. major*, *Try. brucei*, *Try. cruzi*, *Tox. gondii*, *Acanthamoeba castellanii* and *Entamoeba invadens* (Besteiro *et al*., 2006; Alvarez *et al*., 2008; Picazarri *et al*., 2008a; Besteiro *et al*., 2011; Moon *et al*., 2011; Li *et al*., 2012) and in organelle removal and maintenance in *Tetrahymena thermophila*, *Try. brucei*, *Tox. gondii*, *Pl. falciparum*, and *Tri. vaginalis* (Kaneda *et al*., 1991; Benchimol, 1999; Herman *et al*., 2008; Besteiro *et al*., 2011; Liu and Yao, 2012; Tomlins *et al*., 2013). In the slime mold *Dictyostelium discoideum*, it has been shown that autophagy is indispensable for starvation-induced cell differentiation to the multicellular stage (Otto *et al*., 2003; Calvo-Garrido and Escalante, 2010). Unlike the protists described earlier, there are at least three exceptional organisms known to apparently lack the Atg8 conjugation system, *Giardia lamblia*, *Cyanidioschyzon merolae* and *Encephalitozoon cuniculi* from Excavata, Archaeplastida and Opisthokonta respectively (Keeling *et al*., 2005; Duszenko *et al*., 2011).

Entamoeba histolytica is a unicellular protozoan parasite that causes amoebic colitis, dysentery and liver abscesses and annually infects approximately 50 million inhabitants of endemic areas, resulting in an estimated 40 000–110 000 deaths (WHO, 1997). The membrane-trafficking system in this organism appears to be as complex as that in higher eukaryotes, based on the extreme diversity of Rab small GTPases present in the genome (104 *rab* genes; Saito-Nakano *et al*., 2005; Nakada-Tsukui *et al*., 2010). Thus, *En. histolytica* poses a primitive eukaryotic model to study diversity and evolution of membrane-trafficking mechanisms (Dacks and Field, 2007; Field *et al*., 2011). Recent genome surveys have shown that nearly all of the major Atg proteins required for autophagy in yeast are conserved in *En. histolytica*, except for Atg 2, 12, 13 and 14 (Nakatogawa *et al*., 2009; Brennand *et al*., 2011; Duszenko *et al*., 2011), suggesting that the Atg8 conjugation system is conserved, but that the Atg5/Atg12 conjugation system may not be functional or highly diverged.

In the related reptilian species *En. invadens*, Atg8-associated autophagosome-like vesicles/vacuoles are constitutively (i.e. even under non-starving conditions) present during the logarithmic growth of trophozoites and during developmental transition from the trophozoite to the dormant cyst stage (Picazarri *et al*., 2008a). However, exact roles of Atg genes and proteins are not well understood in this primitive eukaryotic lineage. In the present study, we investigated whether the Atg8 conjugation system is specifically involved in autophagy in *En. histolytica* or if it also plays more general and diverse roles in vesicular trafficking. We demonstrated the roles of Atg8 in *En. histolytica* by examining a strain in which Atg8 expression was repressed by small antisense RNA-mediated transcriptional gene silencing.

Results and discussion

Two isotypes of Atg8 are constitutively and ubiquitously expressed and lipid conjugated in En. histolytica

The *En. histolytica* genome contains two *atg8* genes, *Ehatg8a* and *Ehatg8b*, which are 94% identical in their encoded amino acid sequences and located on different positions in the genome (EHI_130660 and EHI_172140). Because flanking sequences including neighbouring genes are totally different, *Ehatg8a* and *Ehatg8b* are not allelic variants. The EhAtg8b isotype contains five additional amino acids (MDPTF) that are not found in EhAtg8a in the amino-terminal region. In addition, these proteins differ by seven other residues: Met6Pro, Glu7Ile, Ser8Asn, Asn49Ser, Glu52Asn, Asp63Gly and Val66Ile (the amino acid in EhAtg8a, the amino acid position and the amino acid in EhAtg8b are shown in this order; amino acid positions correspond to EhAtg8b).

Immunoblot analysis of trophozoite lysates using a polyclonal EhAtg8 antibody raised against recombinant EhAtg8a revealed four bands ranging in size from 14 to 15 kDa (Fig. 1A). The two upper and two lower bands were also detected in the 100 000× *g* soluble protein and pellet fractions and appeared to correspond to the size of the cytosolic and membrane-associated forms, respectively, of EhAtg8a and EhAtg8b. The calculated molecular masses of the EhAtg8a and EhAtg8b isotypes are 14.2 and 14.7 kDa respectively. These data suggest that the two upper and two lower bands in the lysate correspond to non-modified cytosolic and phospholipid-modified membrane-anchored Atg8 isotypes respectively. The expression of both isotypes of the *EhAtg8* gene was confirmed by reverse transcriptase polymerase chain reaction (RT-PCR) and digestion of the amplified fragments with VspI, which recognizes only the *EhAtg8b* amplicon (Fig. S2). EhAtg8s does not have transmembrane domain and the carboxyl-terminal glycine residue known to conjugate to lipids is conserved in EhAtg8s. It is considered that EhAtg8s are also modified with lipids.

We next examined if the expression or distribution of EhAtg8 changed during the *in vitro* culture of trophozoites by performing immunoblot analysis with anti-EhAtg8 antibody and strain as a reference. EhAtg8 was constitutively expressed in *En. histolytica* HM-1:IMSS cl 6 strain (HM-1) irrespective of growth phase (Fig. 1B). The 14.2- and 14.7-kDa bands corresponding to membrane-associated EhAtg8a and b, respectively, were predominantly observed at all examined time points (days 1–5). After 4 days of cultivation, the intensity of the two bands

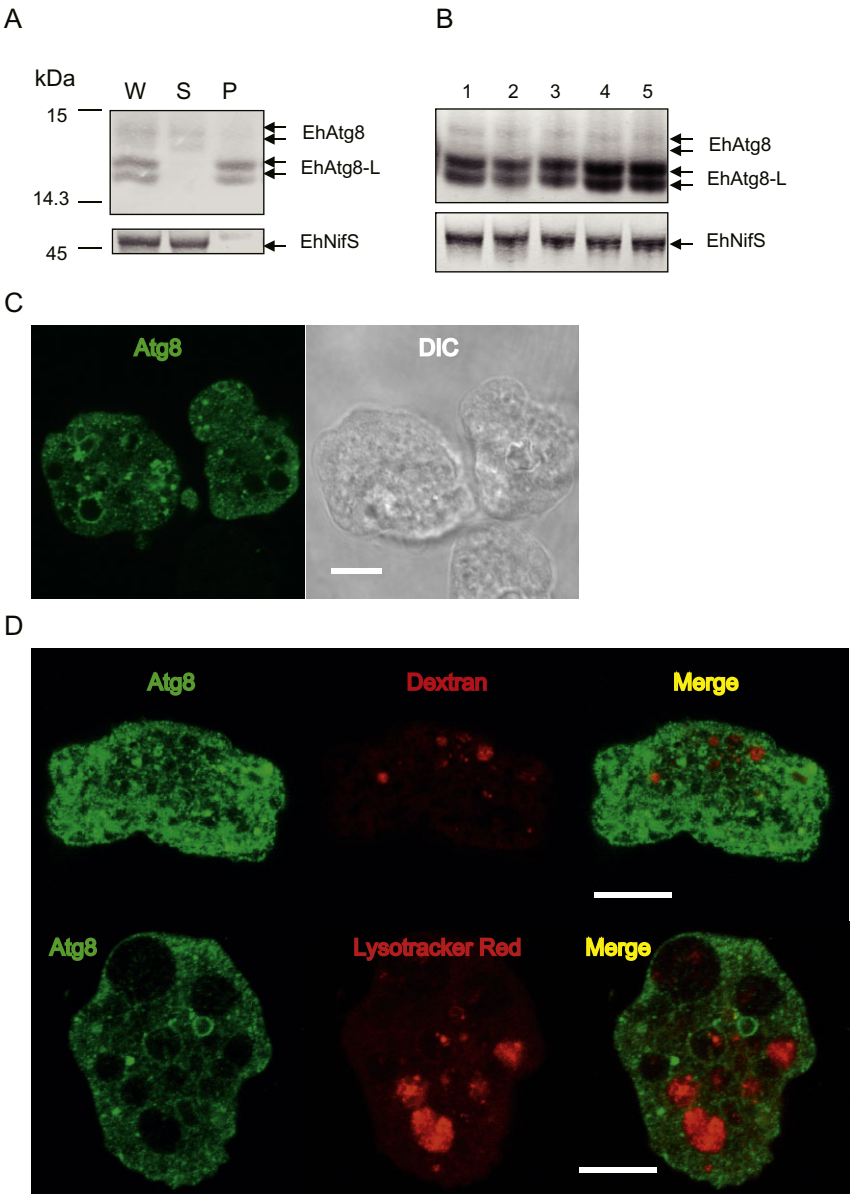

Fig. 1. Immunoblot analysis and cellular localization of Atg8 in *Entamoeba histolytica* trophozoites.
A. Cellular distribution of Atg8. Trophozoites of the HM-1 strain were harvested after 2 days of passage, lysed by mechanical homogenization and centrifuged at 100 000× *g* to separate the supernatant and pellet fractions. The obtained fractions (5 μg) were subjected to immunoblot analysis using anti-EhAtg8 (top) or anti-EhNifS (cytosolic control) antibodies. P, pellet; S, supernatant; W, whole lysate. Unmodified ('EhAtg8') and lipid-modified forms ('EhAtg8-L') are indicated.
B. Immunoblot analysis of EhAtg8 during axenic cultivation. Trophozoites were cultured axenically in BI-S-33 medium for 1, 2, 3, 4 or 5 days (lanes 1–5, respectively). Approximately 5 μg of the whole cell lysate was separated by SDS-PAGE, blotted, reacted with anti-EhAtg8 antibody and developed by chemiluminescence. Arrows indicate unmodified (two top bands) and lipid-modified (two bottom bands) EhAtg8.
C. Localization of EhAtg8 in *En. histolytica* trophozoites. Trophozoites in steady state were fixed and stained for EhAtg8. Bar, 10 μm.
D. Localization of EhAtg8 with FITC-dextran (endosomes) and LysoTracker Red (lysosomes). *En. histolytica* trophozoites were co-cultured with 2 mg mL^{-1} FITC-dextran for 60 min or LysoTracker Red stain and then fixed. Cells were stained for EhAtg8 using anti-EhAtg8 polyclonal antibody. Bars, 10 μm.

increased by ~60%, as determined by densitometric scanning of immunoblots and comparison with EhNifS protein as a reference (Fig. 1B). Immunofluorescence assay also showed that Atg8 was constitutively expressed at all time points (data not shown) and localized throughout the cytoplasm to vesicular/vacuolar and dot-like structures (Fig. 1C), which were similar to the Atg8-associated structures previously observed in *En. invadens* (Picazarri *et al.*, 2008a). Localization of EhAtg8 to endosomes and lysosomes was also examined, but was hardly observed (Fig. 1D). Together, these data suggest that Atg8 plays a role in *En. histolytica* in nutrient-rich, *in vitro* culture conditions and increases slightly in concentration after 4 days of cultivation.

We next verified if Atg8 is also present as two isotypes and lipid-modified in clinical isolates of *En. histolytica*. Immunoblot assays showed that all eight clinical isolates showed a similar pattern of Atg8 staining with anti-EhAtg8 antibody as the HM-1 reference strain (Fig. S3), suggesting that EhAtg8 is also constitutively expressed and lipidated in proliferating trophozoites of all clinical isolates tested.

Multiplication of Atg8 isotypes in Entamoeba *and other organisms*

Atg8 family proteins have two domains, an amino-terminal helical domain (NHD) and a carboxyl-terminal

ubiquitin-like domain (ULD) (Paz *et al*., 2000; Coyle *et al*., 2002; Sugawara *et al*., 2004; Nakatogawa *et al*., 2007). The NHD consists of two alpha helices, which are located at amino acid 1–24 in yeast Atg8. The amino-terminal region containing the five amino acid extensions and three amino acid substitutions unique to EhAtg8b are located within the NHD, while four amino acid substitutions are found within the ULD. As the NHD may play a role in the membrane fusion activity of Atg8 (Weidberg *et al*., 2011), the heterogeneity in this domain between the two EhAtg8 isotypes may affect the fusion activity and localization of Atg8 to membranes. Other *Entamoeba* species, including *Entamoeba dispar* and *Entamoeba moshkovskii*, also have two Atg8 genes (Fig. S1A). In *En. invadens* and *Entamoeba nuttalli*, we identified a protein related to Atg8a, but failed to detect a homolog of Atg8b. Among the four amino acid substitutions in the ULD of EhAtg8b, the Asp58Gly substitution is of particular interest because Asp58 is highly conserved among all Atg8 homologues in *Entamoeba* and a wide range of other organisms, including yeast, human GABARAP, *D. discoideum*, *Tet. thermophila* and *Try. brucei*, suggesting that EhAtg8b may have a unique function (Fig. S1B). However, it remains unknown whether the amino acid differences between the two EhAtg8 isotypes influence membrane fusion activity.

Among protists that have the Atg8 conjugation system, evidence for expansion of Atg8 gene paralogs has been found in *L. major* and *Paramecium tetraurelia*, but not in related species, for example, *Trypanosoma* or *Tetrahymena*. *L. major* possesses 25 Atg8 genes. It was shown that the subgroup of *L. major* Atg8 are not involved in macroautophagy but involved in endocytosis and exocytosis (Krishnamurthy *et al*., 2005; Williams *et al*., 2009). This illustrates a case of gene multiplication and functional diversification of Atg8 (Furuta *et al*., 2002; Baisamy *et al*., 2009; Popovic *et al*., 2012).

Atg8 is not modulated during starvation

We further examined if expression, lipid modifications and localization of EhAtg8 are induced during starvation. Immunoblotting analysis of lysates from amoebas subjected to glucose deprivation and osmolarity shock using 47% low-glucose (LG) medium, which is known to induce encystation in *En. invadens* (Sanchez *et al*., 1994; Picazarri *et al*., 2008a), did not detect any marked changes in either the amount or patterns of EhAtg8 expression (data not shown). These results indicate that these environmental changes do not alter expression, modifications and localization of EhAtg8. In *En. invadens*, lipid-modified Atg8 proteins have a role in encystation (Picazarri *et al*., 2008a). Because laboratory *En. histolytica* strains do not encyst *in vitro* in general, we could not directly test if EhAtg8 is also involved in the encystation. Thus, we cannot conclude that the lipid-anchored membrane-associated form of Atg8 plays an analogous role in *En. invadens* and *En. histolytica*.

Repression of Atg8 *gene expression impairs growth*

To better understand the role of Atg8 in *En. histolytica*, we created a transformant line (Atg8gs) in which EhAtg8 expression was repressed by gene silencing (Bracha *et al*., 2006; Mi-ichi *et al*., 2011; Nakada-Tsukui *et al*., 2012). Immunoblot analysis confirmed > 95% repression of EhAtg8 expression in the Atg8gs transformant compared with the parental G3 strain transformed with an empty vector (Fig. 2A). Indirect immunofluorescence analysis of the Atg8gs line confirmed that the formation of Atg8-associated structure was abolished (Fig. 2B). These data indicate that expression of both *Ehatg8a* and *b* genes was repressed by gene silencing.

To examine if Atg8 plays a role in proliferation, as was previously suggested for *En. invadens* (Picazarri *et al*., 2008a), the growth kinetics of the Atg8gs and control transformants were compared in axenic BI-S-33 medium (Fig. 2C). The growth of the Atg8gs transformant showed a significant reduction of 43–47% after 144 h of culture when compared with the control transformant ($P \leq 0.001$). To test if the growth retardation was due to nutrient starvation, the culture medium was replaced daily to provide an excess amount of nutrients, including free lipids, amino acids and nucleic acids. However, the medium replenishment did not rescue the growth retardation of the Atg8gs transformant (data not shown). Together, these data suggest that Atg8 may be involved in a fundamental cellular process(es), such as the incorporation, scavenging and intracellular trafficking of nutrients.

Atg8 gene silencing inhibits incorporation of a fluid-phase marker and acidification of endosomes and phagosomes

To test the possibility that growth retardation caused by *Ehatg8* gene silencing was due to defect in nutrient uptake and/or degradation, the endocytic rate of the fluid-phase marker fluorescein isothiocyanate (FITC)-dextran and acidification of the compartment containing FITC-dextran was measured. The EhAtg8gs strain showed reduced endocytosis of FITC-dextran (Fig. 3A). After 2 and 3 h of cocultivation with FITC-dextran, EhAtg8gs showed approximately 20% and 15% decreases, respectively, in the amount of incorporated FITC when compared with the pSAP2 control strain ($P \leq 0.001$, Fig. 3A). The percentage of FITC-dextran incorporated in the acidified compartments, that is, late endosomes and lysosomes, was also estimated based on the spectral changes of

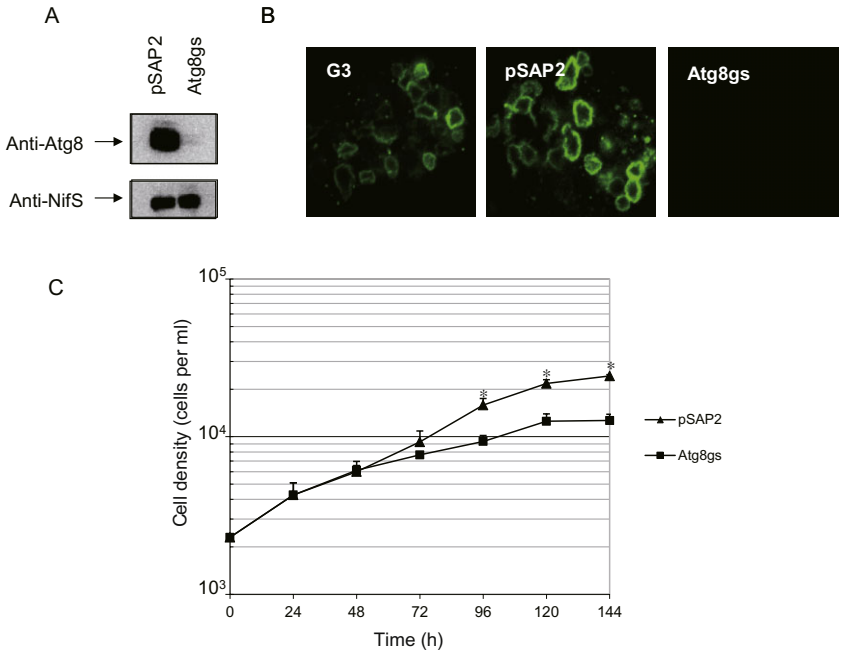

Fig. 2. Phenotypes caused by repression of Atg8 expression in the *EhAtg8*-gene silenced strain.
A. Immunoblot analysis of Atg8. Trophozoites of the *EhAtg8*-gene silenced transformant (Atg8gs) and a control transformant containing empty vector (pSAP2) were harvested after reaching semi-confluency. Approximately 10 μg of whole lysate was separated by SDS-PAGE, blotted onto nitrocellulose membrane and reacted with anti-EhAtg8 or anti-EhNifS antibody. The reacted bands were developed with chemiluminescence.
B. Immunofluorescence images of EhAtg8-associated structures in the parental strain (G3) and pSAP2 and Atg8gs transformants. Representative images with maximal projection are shown.
C. Growth kinetics of pSAP2 and Atg8gs transformants in axenic culture. Axenic cultures were initiated at 2.3×10^3 trophozoites per ml and the cell density was measured at the indicated time points in triplicate. Bars indicate standard deviations. The data shown are a representative result of three independent experiments. Asterisks indicate $P \leq 0.001$.

FITC in response to low pH (Meza and Clarke, 2004; Mitra *et al*., 2005; 2006). After 30 to 120 min of endocytosis, the percentage of acidified endosomes containing incorporated FITC-dextran was significantly lower (16–31%) in the Atg8gs strain compared with the control ($P < 0.05$; Fig. 3B). At 180 min of endocytosis, however, the difference in the percentage of acidified endosomes containing incorporated FITC-dextran between the Atg8gs and control strains decreased (Fig. 3B). This can be explained by two possible reasons: first, there are multiple pathways for lysosome biogenesis, that is biosynthetic and endocytic pathways, as previously suggested (Saftig and Klumperman, 2009) and at the later time point, Atg8-independent pathway compensated the defect and led to the acidification of endosomes in the Atg8gs strain. Second, in the wild-type strain, neutralization of some endosomes already occurred at 180 min of endocytosis. These two concurrent events probably masked the defect in the endosome acidification in Atg8gs strain. Altogether, these data suggest that Atg8 plays a role in fluid-phase endocytosis and the acidification of endosomes.

We further examined whether EhAtg8 is also involved in the acidification of phagosomes. EhAtg8gs and control strains were co-incubated with *Escherichia coli* cells conjugated with pHrodo, which is a fluorogenic dye responsive to acidification, and intracellular fluorescence was analysed. The fluorescent signal attributable to *Es. coli* cells in acidified compartments was markedly lower in the Atg8gs strain compared with the control at all examined time points and the difference reached the level of significance after 30 and 60 min of co-cultivation ($P < 0.04$ and $P < 0.02$ respectively; Fig. 4A). In contrast, the rate of phagocytosis of tetramethylrhodamine isothiocyanate (TRITC)-labelled *Es. coli* and carboxylated beads was only marginally affected in the Atg8gs strain (Fig. 4B and C). The localization of EhAtg8 during phagocytosis was also examined using CellTracker Blue-loaded Chinese hamster ovary (CHO) cells (Fig. 5). The percentage of EhAtg8 localization to phagosomes was 50, 23 and 9.6% after 10, 30 and 60 min of co-cultivation with CHO cells respectively. EhAtg8 was often (77%, $n = 31$) associated with the phagocytic cup at the initiation of ingestion (Fig. 6 and Fig. S5). Together, these data suggest that EhAtg8 is involved in the early phase of phagocytosis and phagosome maturation, more specifically in the acidification of phagosomes.

Initial recruitment of Rab7A/ vacuolar protein sorting 26 (Vps26) to CHO cell-containing phagosomes is not affected by Atg8 repression

The observed inhibition of the endosome and phagosome acidification was possibly caused by a defect in the recruitment of machinery needed for maturation of endosomes/phagosomes. To see the effect of Atg8gs on the recruitment of the key factor(s) of endosome/lysosome acidification, we examined the recruitment of Vps26 to phagosomes in pSAP2 and Atg8gs transformants (Fig. 6). Vps26 is a component of the retromer complex, the downstream effector of Rab7A small GTPase, and well colocalized with Rab7A. It has been previously shown that Rab7A and Vps26 are the major regulator of acidification of endosomes,

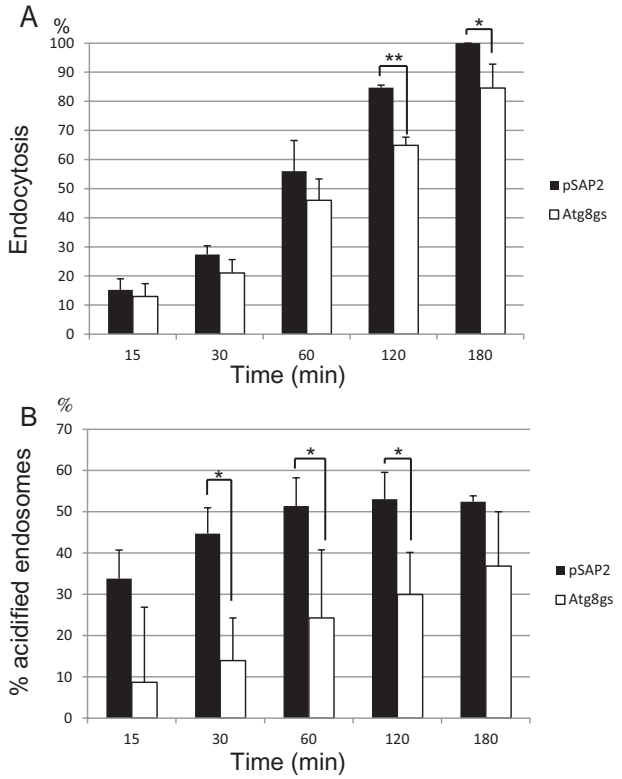

Fig. 3. Atg8 suppression delayed endocytosis and endosome acidification. Trophozoites of the pSAP2 and Atg8gs transformants were incubated with 2 mg ml^{-1} FITC-dextran for 15, 30, 60, 120 and 180 min and then harvested. Endocytosis efficiency is shown as the percentage of incorporated FITC-dextran relative to the fluorescence intensity measured at the neutral pH for the control pSAP2 transformant after 180 min.
A. Total fluorescence signal measured in whole cell lysates (at neutral pH) of pSAP2 and Atg8gs strains. The fluorescence signal of the lysate of the control (pSAP2) cells incubated with FITC-dextran for 180 min was set as 100%. The average values of three independent experiments are shown. Note that the fluorescence intensity indicates the total amount of incorporated FITC-dextran.
B. The percentage of acidified endosomes in pSAP2 and Atg8gs transformants. The percentage of acidified endosomes at each time point was calculated using the following equation: percentage of acidified endosomes equals [(fluorescent signal from the whole lysate) minus (fluorescent signal from the cell suspension)] divided by (fluorescent signal from the whole lysate). $^{**}P < 0.001$; $^{*}P < 0.05$ by Student's *t*-test.

lysosomes and phagosomes and also of the transport of cysteine proteases (Nakada-Tsukui *et al.*, 2005). It has been previously shown that during erythrophagocytosis, Rab7A is recruited to phagosomes at the late time point (30 min), via pre-phagosomal vacuoles, which are associated with both Rab5 and Rab7A and formed at early time points (5–10 min) prior to full maturation of phagosomes (Saito-Nakano *et al.*, 2004). Vps26 well colocalizes with Rab7A (Saito-Nakano *et al.*, 2004; Nakada-Tsukui *et al.*, 2005) and is recruited to phagosomes at around 30 min.

Slightly different from the previous observation on erythrophagocytosis (Saito-Nakano *et al.*, 2004), Vps26 was recruited to the phagocytic cups and phagosomes during ingestion of CHO cells at as early as 10 min in the control cells (pSAP2 strain with G3 background). When the unclosed phagocytic cups were examined in pSAP2 strain at 10 min, approximately 83% of them (30 of 36) were associated with Atg8, but only 28% (9 of 36) were

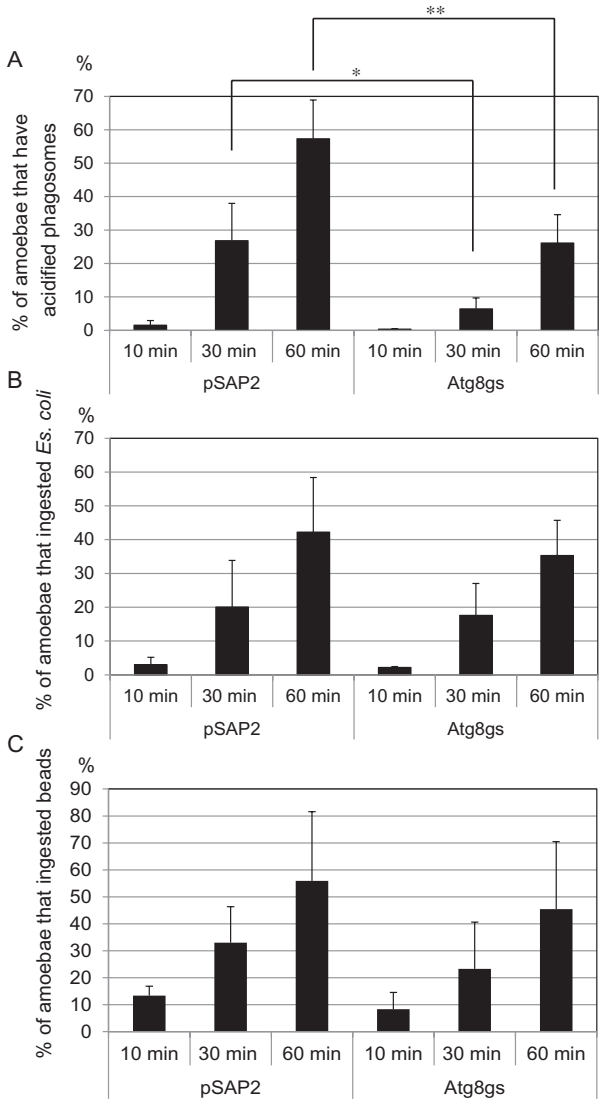

Fig. 4. Atg8 suppression delayed phagosome acidification, but not phagocytosis.
Trophozoites of the pSAP2 and Atg8gs transformants were co-cultured with pHrodo-labelled *Es. coli* (A), TRITC-labelled *Es. coli* (B) or Nile Red-labelled carboxylate-modified FluoSphere microspheres (C) for the indicated time. The percentage of trophozoites that ingested stained cells and/or microspheres was determined by flow cytometry (FACS) and the percentage of fluorescence phagosomes are shown. $^{**}P < 0.02$; $^{*}P < 0.04$ by Student's *t*-test.

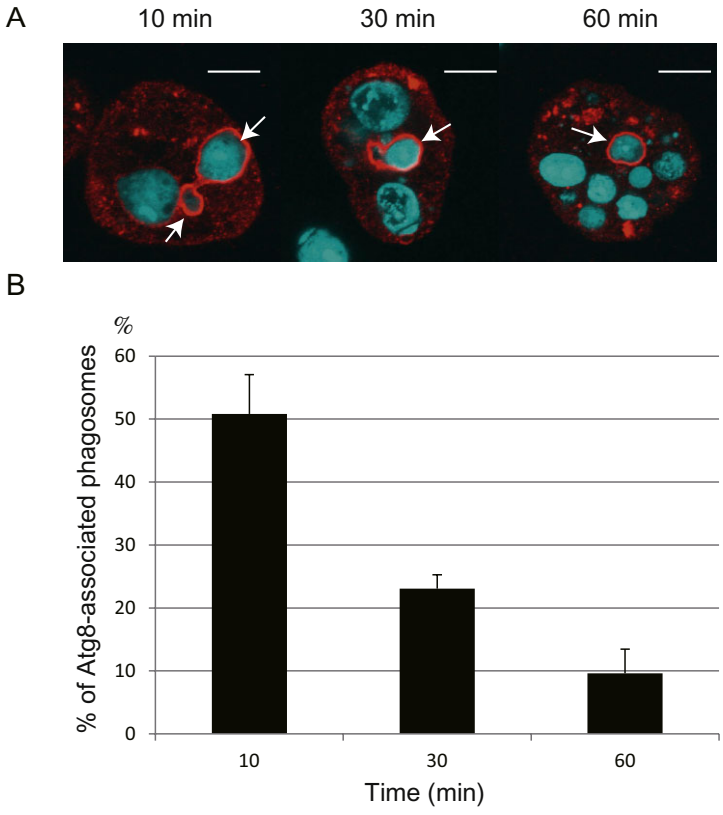

Fig. 5. Localization of Atg8 on the phagosome membrane.
A. *Entamoeba histolytica* trophozoites of strain HM-1 were co-cultured with CellTracker Blue-loaded CHO cells for the indicated times, fixed and then reacted with anti-EhAtg8 antibody and Alexa-568 conjugated anti-rabbit IgG secondary antibody. Arrows indicate phagosomes with EhAtg8.
B. Percentage of phagosomes associated with EhAtg8. At 10, 30 or 60 min after co-cultivation, phagosomes were counted (approximately 40, 100 or 180 phagosomes, respectively) and the percentage of phagosomes that were associated with EhAtg8 was calculated. The average values of three independent experiments are shown.

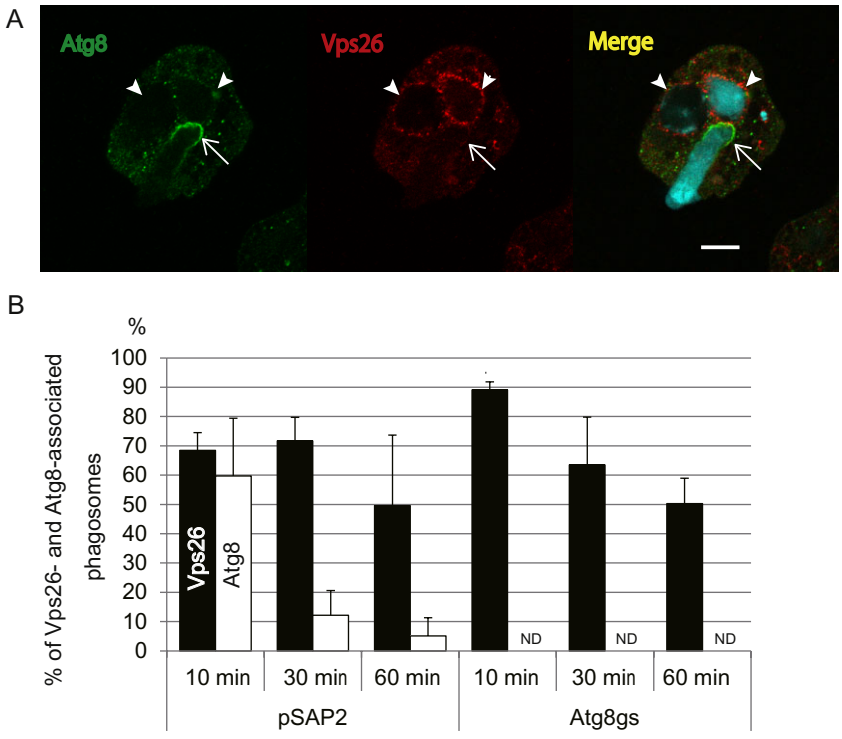

Fig. 6. Recruitment of Vps26 and Atg8 to phagosomes and the phagocytic cups.
Entamoeba histolytica trophozoites of pSAP2 and Atg8gs transformants were co-cultured with CellTracker Blue-loaded CHO cells for the indicated times, fixed and then reacted with anti-EhAtg8 and anti-EhVps26 antibodies labelled with Alexa Fluor 488 or Alexa Fluor 546 by ZENON rabbit IgG labelling kit.
A. Localization of Atg8 and Vps26 in *En. histolytica* pSAP2 control trophozoites. One representative cell was shown (see Fig. S5 for additional cells). White arrow indicates Atg8-positive, Vps26-negative, unclosed phagocytic cup and white arrowheads indicate Vps26-associated, but Atg8-negative phagosomes.
B. The percentage of phagosomes associated with EhAtg8 (open bars) or Vps26 (filled bars). At 10, 30 or 60 min after co-cultivation, phagosomes were examined and the percentage of phagosomes that were associated withEhAtg8 and EhVps26 was calculated. Atg8 association was not determined in Atg8gs strains (ND). Averages of three independent experiments are shown.

associated with Vps26 (data not shown; typical image is shown in Fig. 6A). On the other hand, when enclosed phagosomes were examined in pSAP2 strain at 10 min, approximately 60% or 70% of them were associated with Atg8 or Vps26 respectively (Fig. 6B). These data are consistent with the premise that the recruitment of Atg8 precedes that of Vps26. The percentage of enclosed phagosomes associated with Vps26 was comparable between pSAP2 and Atg8gs (Fig. 6B). These data suggest that although Atg8 is recruited to the phagocytic cup prior to Vps26, the presence of Atg8 is not prerequisite for further recruitment of Vps26. Furthermore, the defect in phagosome acidification caused by Atg8gs is not due to interference with the Rab7A/Vps26-dependent pathway. Taken together, Atg8 is involved in the initial phase of phagosome acidification in a Rab7A/Vps26-independent fashion.

Role of Atg8 in endosome and phagosome maturation in En. histolytica

A recent genome survey of 20 protists, including *D. discoideum*, *Acanthamoeba* spp., *L. major*, *Try. brucei*, *Try. cruzi*, *Tox. gondii*, *Pl. falciparum* and *Plasmodium berghei*, revealed that Atg genes are highly conserved among protozoa (Duszenko *et al.*, 2011). Among parasitic protozoa, molecular mechanisms of autophagy have been well studied in the trypanosomatid and apicomplexan parasites *L. major*, *Try. brucei*, *Try. cruzi* and *Tox. gondii* (Besteiro *et al.*, 2006; 2011; Alvarez *et al.*, 2008; Koopmann *et al.*, 2009; Li *et al.*, 2012). In these parasites, autophagy is important for stage conversion and is also likely involved in organelle removal during stage transition. Despite the conservation of core Atg genes of the Atg8 conjugation system, however, their roles in individual protozoa need to be experimentally validated. As shown here, EhAtg8 is apparently involved in lysosome/phagosome acidification and is less likely to play a role in stress responses, such as nutrient starvation. This finding was unexpected because Atg8 in *En. invadens* was previously demonstrated to be involved in stage conversion, which is closely associated with stress responses (Picazarri *et al.*, 2008a). Numerous molecules play a role in phagocytosis and phagosome maturation in *En. histolytica* and include Rab small GTPases, the retromer complex, CaBP1, CaBP3, EhFP4, phosphatidylinositol 3-phosphate (PtdIns3P) and phosphatidylinositol 4-phosphate (PtdIns4P). Among them, Rab small GTPases, the retromer complex, PtdIns3P and PtdIns4P are considered to be involved in phagosome maturation (Saito-Nakano *et al.*, 2004; 2007; Marion *et al.*, 2005; Nakada-Tsukui *et al.*, 2005; 2009; 2010; 2012; Okada *et al.*, 2005; Okada *et al.*, 2006; Jain *et al.*, 2008; Somlata *et al.*, 2011). PtdIns3P is also a key molecule that determines the site of Atg8 lipidation via the recruitment of the Atg5-Atg12 : Atg16L complex in mammalian cells (Fujita *et al.*, 2008). It was also suggested that PtdIns3P plays a pivotal role in the generation of light chain 3 (LC3)-associated phagosomes, in which PtdIns3P synthesis occurs before LC3 recruitment, based on the results of live-cell imaging of entosis in mammals and apoptotic degradation of Q neuroblast lineage cells in *Caenorhabditis elegans* (Florey *et al.*, 2011; Li *et al.*, 2012). We previously reported that PtdIns3P is generated or recruited on phagosomal membranes during the phagocytic cup formation and in the very early phase of phagocytosis in *En. histolytica* (Nakada-Tsukui *et al.*, 2009). Specifically, the percentage of PtdIns3P-associated phagosomes (69 ± 6.7, 51 ± 4.5 and 27 ± 5.7% after 10, 30 and 60 min of co-cultivation with CHO cells, respectively; Nakada-Tsukui *et al.*, 2009) was found to be higher than that of Atg8-associated phagosomes (50 ± 8.3, 23 ± 2.3, and 9 ± 3.4%, respectively), as shown in the present study. These data suggest that the generation/recruitment of PtdIns3P to the phagosomal membrane precedes the recruitment of Atg8. In this report, we have also shown by the kinetic study of the recruitment of Atg8 and Vps26/Rab7A that Atg8 is involved in the initial phase of the formation of the phagocytic cup, similar to PtdIns3P, and their further maturation in a Rab7A-independent pathway (Fig. 6). It is important to investigate where and how PtdIns3P is involved in the recruitment of Atg8 during the phagosome formation in a future study.

In conclusion, the findings from our present study demonstrate that Atg8 is involved in lysosomal and phagosomal acidification, a process that is required for the activation of hydrolases such as cysteine proteases, which are well established virulence factors in *En. histolytica* (Hellberg *et al.*, 2001; Tillack *et al.*, 2006; Mitra *et al.*, 2007; Matthiesen *et al.*, 2013). Further investigation into the unique role and regulatory mechanisms of Atg8 in *En. histolytica* may help identify novel, unique targets to develop effective measures against this important protozoan pathogen.

Experimental procedures

Bacteria, chemicals and reagents

Escherichia coli DH5α and BL21 (DE3) strains were purchased from Life Technologies (Tokyo, Japan) and Invitrogen (C6000-03) respectively. All chemicals of analytical grade were purchased from Sigma-Aldrich (Tokyo, Japan) or Wako (Tokyo, Japan) unless otherwise stated.

En. histolytica *strains and culture*

Trophozoites of *En. histolytica* strain HM-1 : IMSS cl6 (HM-1) were cultured axenically in BI-S-33 medium (Diamond *et al.*,

1978) at 35.5°C, as previously described (Clark and Diamond, 2002). An *En. histolytica* clinical isolate, KU45 (zymodeme XIV), was isolated from stool of a dysenteric patient in Urayasu, Chiba, Japan in April 2004. KU46 (II) was isolated from a diarrhoeal patient resistant to metronidazole treatment in Hamamatsu, Shizuoka, Japan in April 2004. KU47 (II) was isolated from an human immunodeficiency virus (HIV)-positive diarrhoeal patient in Tokyo, Japan in April, 2004. KU48 (XIV) was isolated from liver aspirates of a patient in Tokyo, Japan in May 2006. KU50 was isolated from a diarrhoeal patient at Bokuto Tokyo Metropolitan Hospital, Tokyo, Japan in March 2007. These clinical isolates were monoxenically cultivated in the presence of *Crithidia fasciculata*, as previously described (Costa *et al*., 2006). KU2, KU3, KU5 and KU13 (Haghighi *et al*., 2002; Nozaki *et al*., 2006) were cultivated in axenic conditions.

Recombinant En. histolytica *Atg8 (*Eh*Atg8) and antiserum against* Eh*Atg8*

Standard techniques were used for routine DNA manipulations, subcloning and plasmid construction (Sambrook and Russell, 2001). Production of recombinant protein encoded by the *EhAtg8a* gene (XP_649165) and antiserum against the EhAtg8a was performed as described previously (Picazarri *et al*., 2008a,b).

RT-PCR

To determine if *EhAtg8a* and *EhAtg8b* were expressed at the mRNA level, RT-PCR with isotype-specific oligonucleotides, *EhAtg8a* sense: 5′-ATAGAATAAATGGAATCACAACCA-3′, *EhAtg8b* sense: 5′-ATGGATCCAACTTTTCCAATAAAC- 3′ and common antisense: 5′-TTAATTTCCAAAGACAGATTCTCT-3′, was conducted as previously described (Mitra *et al*., 2007). Briefly, polyadenylated RNA was extracted from HM-1 trophozoites with a Messenger RNA Isolation Kit (Agilent Technologies, Tokyo, Japan) and then treated with deoxyribonuclease I (Invitrogen, 18047-019) to exclude genomic DNA. Poly-A RNA was reverse transcribed with the SuperScript III First-Strand Synthesis System and oligo$(dT)_{20}$ primer (Invitrogen, 18080051). PCR was performed with the resulting cDNA as a template using a DNA Engine Peltier Thermal Cycler (Bio-Rad, Hercules, CA, USA). The PCR cycling conditions consisted of an initial step of denaturation at 94°C for 1 min, followed by 30 cycles of denaturation at 98°C for 10 s, annealing at 52°C for 30 s and extension at 72°C for 30 s.

Gene silencing of EhAtg8

Gene silencing was performed as previously described (Bracha *et al*., 2006; Mi-ichi *et al*., 2011; Nakada-Tsukui *et al*., 2012). Briefly, a 384-bp fragment containing the entire open reading frame (ORF) of *EhAtg8a* gene starting at the initiation codon was amplified by PCR with the oligonucleotide primers 5′-aaaaggcctATGGAATCACAACCAAAACTT-3′ and 5′- ggggagctc TTAATTTCCAAAGACAGATTC-3′ using pGST-EhAtg8 as a template (Picazarri *et al*., 2008a). The PCR cycling conditions consisted of 98°C for 30 s, followed by 30 cycles of 98°C for 5 s, 55°C for 20 s, 72°C for 30 s and a final extension at 75°C for 5 min. The obtained PCR product was digested with StuI and SacI and inserted into StuI/SacI-digested pSAP2 45 to produce pEhATG8gs. This plasmid was introduced into the *En. histolytica* G3 strain (Bracha *et al*., 2003; 2006) by liposome-mediated transfection (Nozaki *et al*., 1999; Picazarri *et al*., 2008b). Transformants were selected and maintained in medium supplemented with 6 μg ml^{-1} geneticin.

Cell fractionation

Approximately 5–7 × 10^6 trophozoites were harvested, washed twice with phosphate-buffered saline (PBS) containing 2% glucose and resuspended in homogenization buffer [50 mM Tris, pH 7.5, 250 mM sucrose, 50 mM NaCl and 1.34 mM trans-epoxysuccinyl-L-leucylamido-(4-guanidino)butane (E-64)]. The amoebae were homogenized with 100 strokes in a glass homogenizer and then centrifuged at 400× *g* for 5 min at 4°C to remove unbroken cells. The supernatant was further centrifuged at 100 000× *g* for 1 h and the obtained pellet and supernatant fractions were subjected to immunoblot analysis and phospholipase D treatment.

Immunoblot analysis

Sodium dodecyl sulfate (SDS)-polyacrylamide gel electrophoresis (PAGE) was conducted using 13.5% separating gels containing 6 M urea as previously described (Kirisako *et al*., 2000). Approximately 5 μg of lysates or membrane fractions were separated by denaturing SDS-PAGE and transferred to nitrocellulose membranes. The membranes were blocked with 5% skim milk in Tris-buffered saline Tween 20 (TBS-T) [50 mM Tris-HCl (pH8.0), 150 mM NaCl, 0.5% Tween20] and were then incubated with anti-EhAtg8 (1:1000 dilution) (Picazarri *et al*., 2008a) or anti-EhNifS (1:1000 dilution) (Ali *et al*., 2004) rabbit polyclonal antibodies overnight at 4°C. After washing in TBS-T, the membranes were incubated with rabbit IgG horseradish peroxidase (HRP)-conjugated antibody (1:10000 dilution) (GE Healthcare, NA934) for 1 h. Reacted bands were visualized by chemiluminescence using the Immobilon Western Chemiluminescent HRP substrate (Millipore Corp., P36599).

Indirect immunofluorescence assay

Trophozoites were fixed with 3.7% paraformaldehyde in PBS (pH 6.6) at room temperature for 10 min, washed with PBS and then permeabilized with 0.2% saponin for 10 min. The permeabilized cells were incubated with anti-EhAtg8 polyclonal rabbit (1:1000 dilution) or anti-HA (1:1000 dilution) mouse monoclonal antibody for 1 h and subsequently incubated with anti-mouse, anti-rabbit IgG Alexa Fluor 488 antibody or anti-mouse IgG Alexa Fluor 568 antibody (Invitrogen, A11029, A11034, A11031) for 1 h at room temperature. Finally, the cells were washed with PBS containing 0.1% bovine serum albumin (BSA), mounted on a slide glass and examined under a confocal laser scanning microscope (Carl Zeiss, LSM 510 META). Images were analysed with LSM 510 software (Carl Zeiss, Jena, Germany).

Endocytosis assay

Approximately 4–5 × 10^5 cells were incubated in 500 μl BI-S-33 medium containing 2 mg ml^{-1} FITC-dextran at 37°C for

15–180 min. Cells were washed twice with cold PBS and resuspended in 500 µl PBS. The fluorescence signal from a 250-µl sample of the cell suspension was measured using a F-2500 Fluorescence Spectrophotometer (Hitachi High-Technologies, Tokyo, Japan) with excitation at 495 nm and emission at 519 nm. The remaining 250 µl of the cell suspension was lysed with 1:10 volume of 10X lysis buffer, and the fluorescence signal and total amount of endocytosed dextran in the lysate was measured as described earlier. As FITC has much stronger fluorescence emission at neutral pH compared with acidic pH, the fluorescence signal from live cells largely reflects the amount of FITC-dextran in non-acidified endosomes, whereas the signal in the lysate at neutral pH indicates the total amount of FITC-dextran in the cell (Meza and Clarke, 2004; Mitra *et al*., 2005; 2006). All assays were performed in duplicate. Endocytosis efficiency was calculated based on the fluorescence from cell lysates that had been neutralized to limit bias from the pH of different cellular compartments. The fluorescence signal of the lysate of the control (pSAP2) cells harvested after 180 min of co-incubation with FITC-dextran was set as 100%. The percentage of acidified endosomes was calculated by dividing the fluorescence signal of the unlysed cell suspension with that of the neutralized cell lysate.

Phagocytosis assay

Approximately 10^5 amoebae were grown overnight in a 24-well plate under anaerobic conditions. Nile Red fluorescent carboxylate-modified FluoSphere microspheres (Molecular Probes,F8825), TRITC-labelled *Es. coli* cells (Molecular Probes, E2862) or pHrodo-labelled *Es. coli* cells (Molecular Probes, P35366) were added to the amoebae. After incubation for 0, 10, 30 or 60 min at 35.5°C, the amoebae were washed once with warm PBS containing 250 mM galactose (PBS-galactose) and 450 µL PBS-galactose was added. The plate was chilled on ice and detached amoebae were recovered and analysed by two-colour flow cytometry (Becton Dickinson, FACSCalibur). To examine the localization of Atg8 during phagocytosis, approximately 3×10^5 of CellTracker Blue-loaded CHO cells were added to each 8-mm well containing 1×10^5 *En. histolytica* trophozoites on a slide glass. After incubation for 10, 30 and 60 min, the cells were fixed and stained with anti-EhAtg8 antiserum and anti-rabbit IgG Alexa Fluor 568 antibody. The stained cells were examined under a LSM510 META microscope, as described earlier. To examine the colocalization of Atg8 and Vps26, fixed cells were stained with Alexa Fluor 488- or Alexa Fluor 546-labelled anti-EhAtg8 and anti-EhVps26 (Nakada-Tsukui *et al*., 2005) rabbit serum by ZENON rabbit IgG labeling kit (Life technologies, Z-25302 and Z-25304) respectively.

Acknowledgements

We are grateful to Dr. Dan Sato (Kyoto Institute of Technology) and Dr. Atsushi Furukawa (Hokkaido University) for recombinant production of EhAtg8 and establishment of EhAtg8-gene silenced strain respectively. We are also grateful to Dr. Isei Tanida (Juntendo University) for helpful suggestions. This work was supported by a Grant-in-Aid for Scientific Research from the Ministry of Education, Culture, Sports, Science and Technology (MEXT) of Japan to T.N. (23117001, 23117005, 14506236) and K.N.-T. (24590513, 26111524), grants for research on emerging and re-emerging infectious diseases from the Ministry of Health, Labour and Welfare of Japan (H26-Shinkojitsuyoka-ippan-009 and H26-Shinkojitsuyoka-ippan-011) to T.N.

References

Ali, V., Shigeta, Y., Tokumoto, U., Takahashi, Y., and Nozaki, T. (2004) An intestinal parasitic protist, *Entamoeba histolytica*, possesses a non-redundant nitrogen fixation-like system for iron-sulfur cluster assembly under anaerobic conditions. *J Biol Chem* **279:** 16863–16874.

Alvarez, V.E., Kosec, G., Sant'Anna, C., Turk, V., Cazzulo, J.J., and Turk, B. (2008) Autophagy is involved in nutritional stress response and differentiation in *Trypanosoma cruzi*. *J Biol Chem* **283:** 3454–3464.

Baisamy, L, Cavin, S, Jurisch, N, Diviani, D. (2009) The ubiquitin-like protein LC3 regulates the Rho-GEF activity of AKAP-Lbc. *J Biol Chem*. **284:** 28232–28242.

Benchimol, M. (1999) Hydrogenosome autophagy: an ultrastructural and cytochemical study. *Biol Cell* **91:** 165–174.

Besteiro, S., Williams, R.A., Morrison, L.S., Coombs, G.H., and Mottram, J.C. (2006) Endosome sorting and autophagy are essential for differentiation and virulence of *Leishmania major*. *J Biol Chem* **281:** 11384–11396.

Besteiro, S., Brooks, C.F., Striepen, B., and Dubremetz, J.F. (2011) Autophagy protein Atg3 is essential for maintaining mitochondrial integrity and for normal intracellular development of *Toxoplasma gondii* tachyzoites. *PLoS Pathog* **7:** e1002416.

Bracha, R., Nuchamowitz, Y., and Mirelman, D. (2003) Transcriptional silencing of an amoebapore gene in *Entamoeba histolytica*: molecular analysis and effect on pathogenicity. *Eukaryot Cell* **2:** 295–305.

Bracha, R., Nuchamowitz, Y., Anbar, M., and Mirelman, D. (2006) Transcriptional silencing of multiple genes in trophozoites of *Entamoeba histolytica*. *PLoS Pathog* **2:** e48.

Brennand, A., Gualdrón-López, M., Coppens, I., Rigden, D.J., Ginger, M.L., and Michels, A. (2011) Autophagy in parasitic protists: unique features and drug targets. *Mol Biochem Parasitol* **177:** 83–99.

Calvo-Garrido, J., and Escalante, R. (2010) Autophagy dysfunction and ubiquitin-positive protein aggregates in *Dictyostelium* cells lacking Vmp1. *Autophagy* **6:** 100–109.

Clark, C.G., and Diamond, L.S. (2002) Methods for cultivation of luminal parasitic protists of clinical importance. *Clin Microbiol Rev* **15:** 329–341.

Costa, A.O., Gomes, M.A., Rocha, O.A., and Silva, E.F. (2006) Pathogenicity of *Entamoeba dispar* under xenic and monoxenic cultivation compared to a virulent *E. histolytica*. *Rev Inst Med Trop Sao Paulo* **48:** 245–250.

Coyle, J.E., Qamar, S., Rajashankar, K.R., and Nikolov, D.B. (2002) Structure of GABARAP in two conformations: implications for GABA(A) receptor localization and tubulin binding. *Neuron* **33:** 63–74.

Dacks, J.B., and Field, M.C. (2007) Evolution of the eukaryotic membrane-trafficking system: origin, tempo and mode. *J Cell Sci* **120:** 2977–2985.

Diamond, L.S., Harlow, D.R., and Cunnik, C.C. (1978) A new medium for the axenic cultivation of *Entamoeba histolytica* and other *Entamoeba*. *Trans R Soc Trop Med Hyg* **72:** 431–432.

Duszenko, M., Ginger, M.L., Brennand, A., Gualdrón-López, M., Colombo, M.-I., Coombs, G.H., *et al*. (2011) Autophagy in protists. *Autophagy* **7:** 127–158.

Field, M.C., Sali, A., and Rout, M.P. (2011) Evolution: on a bender–BARs, ESCRTs, COPs, and finally getting your coat. *J Cell Biol* **193:** 963–972.

Florey, O., Kim, S.E., Sandoval, C.P., Haynes, C.M., and Overholtzer, M. (2011) Autophagy machinery mediates macroendocytic processing and entotic cell death by targeting single membranes. *Nat Cell Biol* **13:** 1335–1343.

Fujita, N., Itoh, T., Omori, H., Fukuda, M., Noda, T., and Yoshimori, T. (2008) The Atg16L complex specifies the site of LC3 lipidation for membrane biogenesis in autophagy. *Mol Biol Cell* **19:** 2092–2100.

Furuta, S, Miura, K, Copeland, T, Shang, WH, Oshima, A, Kamata, T. (2002) Light Chain 3 associates with a Sos1 guanine nucleotide exchange factor: its significance in the Sos1-mediated Rac1 signaling leading to membrane ruffling. *Oncogene* **21:** 7060–7066.

Haghighi, A., Kobayashi, S., Takeuchi, T., Masuda, G., and Nozaki, T. (2002) Remarkable genetic polymorphism among *Entamoeba histolytica* isolates from a limited geographic area. *J Clin Microbiol* **40:** 4081–4090.

Hellberg, A., Nickel, R., Lotter, H., Tannich, E., and Bruchhaus, I. (2001) Overexpression of cysteine proteinase 2 in *Entamoeba histolytica* or *Entamoeba dispar* increases amoeba-induced monolayer destruction *in vitro* but does not augment amoebic liver abscess formation in gerbils. *Cell Microbiol* **3:** 13–20.

Herman, M., Pérez-Morga, D., Schtickzelle, N., and Michels, P.A.M. (2008) Turnover of glycosomes during life-cycle differentiation of *Trypanosoma brucei*. *Autophagy* **4:** 294–308.

Jain, R., Santi-Rocca, J., Padhan, N., Bhattacharya, S., Guillen, N., and Bhattacharya, A. (2008) Calcium-binding protein 1 of *Entamoeba histolytica* transiently associates with phagocytic cups in a calcium-independent manner. *Cell Microbiol* **10:** 1373–1389.

Kabeya, Y., Mizushima, N., Ueno, T., Yamamoto, A., Kirisako, T., Noda, T., *et al*. (2000) LC3, a mammalian homologue of yeast Apg8p, is localized in autophagosome membranes after processing. *EMBO J* **19:** 5720–5728.

Kaneda, Y., Torii, M., Tanaka, T., and Aikawa, M. (1991) *In vitro* effects of berberine sulphate on the growth and structure of *Entamoeba histolytica*, *Giardia lamblia* and *Trichomonas vaginalis*. *Ann Trop Med Parasitol* **85:** 417–425.

Keeling, P.J., Burger, G., Durnford, D.G., Lang, B.F., Lee, R.W., Pearlman, R.E., *et al*. (2005) The tree of eukaryotes. *Trends Ecol Evol* **20:** 670–676.

Kirisako, T., Ichimura, Y., Okada, H., Kabeya, Y., Mizushima, N., Yoshimori, T., *et al*. (2000) The reversible modification regulates the membrane-binding state of Apg8/Aut7 essential for autophagy and the cytoplasm to vacuole targeting pathway. *J Cell Biol* **151:** 263–276.

Komatsu, M., and Ichimura, Y. (2010) Physiological significance of selective degradation of p62 by autophagy. *FEBS Lett* **584:** 1374–1378.

Koopmann, R., Muhammad, K., Perbandt, M., Betzel, C., and Duszenko, M. (2009) *Trypanosoma brucei* ATG8: structural insights into autophagic-like mechanisms in protozoa. *Autophagy* **5:** 1085–1091.

Krishnamurthy, G., Vikram, R., Singh, S.B., Patel, N., Agarwal, S., Mukhopadhyay, G., *et al*. (2005) Hemoglobin receptor in *Leishmania* is a hexokinase located in the flagellar pocket. *J Biol Chem* **280:** 5884–5891.

Li, W., Zou, W., Yang, Y., Chai, Y., Chen, B., Cheng, S., *et al*. (2012) Autophagy genes function sequentially to promote apoptotic cell corpse degradation in the engulfing cell. *J Cell Biol* **197:** 27–35.

Liu, M.L., and Yao, M.C. (2012) Role of ATG8 and autophagy in programmed nuclear degradation in *Tetrahymena thermophila*. *Eukaryot Cell* **11:** 494–506.

Loos, B., Engelbrecht, A.M., Lockshin, R.A., Klionsky, D.J., and Zakeri, Z. (2013) The variability of autophagy and cell death susceptibility: unanswered questions. *Autophagy B* **9:** 1270–1285.

Marion, S., Laurent, C., and Guillén, N. (2005) Signalization and cytoskeleton activity through myosin IB during the early steps of phagocytosis in *Entamoeba histolytica*: a proteomic approach. *Cell Microbiol* **7:** 1504–1518.

Matthiesen, J., Bär, A.K., Bartels, A.K., Marien, D., Ofori, S., Biller, L., *et al*. (2013) Overexpression of specific cysteine peptidases confers pathogenicity to a nonpathogenic *Entamoeba histolytica* clone. *MBio* **4:** pii: e00072-13. doi: 10.1128/mBio.00072-13.

Mehrpour, M., Esclatine, A., Beau, I., and Codogno, P. (2010) Autophagy in health and disease. 1. Regulation and significance of autophagy: an overview. *Am J Physiol Cell Physiol* **298:** C776–C785.

Meza, I., and Clarke, M. (2004) Dynamics of endocytic traffic of *Entamoeba histolytica* revealed by confocal microscopy and flow cytometry. *Cell Motil Cytoskeleton* **59:** 215–226.

Mi-ichi, F., Makiuchi, T., Furukawa, A., Sato, D., and Nozaki, T. (2011) Sulfate activation in mitosomes plays an important role in the proliferation of *Entamoeba histolytica*. *PLoS Negl Trop Dis* **5:** e1263.

Mitra, B.N., Yasuda, T., Kobayashi, S., Saito-Nakano, Y., and Nozaki, T. (2005) Differences in morphology of phagosomes and kinetics of acidification and degradation in phagosomes between the pathogenic *Entamoeba histolytica* and the non-pathogenic *Entamoeba dispar*. *Cell Motil Cytoskeleton* **62:** 84–99.

Mitra, B.N., Kobayashi, S., Saito-Nakano, Y., and Nozaki, T. (2006) *Entamoeba histolytica*: differences in phagosome acidification and degradation between attenuated and virulent strains. *Exp Parasitol* **114:** 57–61.

Mitra, B.N., Saito-Nakano, Y., Nakada-Tsukui, K., Sato, D., and Nozaki, T. (2007) Rab11B small GTPase regulates secretion of cysteine proteases in the enteric protozoan parasite *Entamoeba histolytica*. *Cell Microbiol* **9:** 2112–2125.

Mizushima, N., and Komatsu, M. (2011) Autophagy: renovation of cells and tissues. *Cell* **147:** 728–741.

Mizushima, N., Yoshimori, T., and Ohsumi, Y. (2011) The role of Atg proteins in autophagosome formation. *Annu Rev Cell Dev Biol* **27:** 107–132.

Moon, E.K., Chung, D.I., Hong, Y., and Kong, H.H. (2011) Atg3-mediated lipidation of Atg8 is involved in encystation of *Acanthamoeba*. *Korean J Parasitol* **49:** 103–108.

Nakada-Tsukui, K., Saito-Nakano, Y., Ali, V., and Nozaki, T. (2005) A retromerlike complex is a novel Rab7 effector that is involved in the transport of the virulence factor cysteine protease in the enteric protozoan parasite *Entamoeba histolytica*. *Mol Biol Cell* **16:** 5294–5303.

Nakada-Tsukui, K., Okada, H., Mitra, B.N., and Nozaki, T. (2009) Phosphatidylinositol-phosphates mediate cytoskeletal reorganization during phagocytosis via a unique modular protein consisting of RhoGEF/DH and FYVE domains in the parasitic protozoon *Entamoeba histolytica*. *Cell Microbiol* **11:** 1471–1491.

Nakada-Tsukui, K., Saito-Nakano, Y., Husain, A., and Nozaki, T. (2010) Conservation and function of Rab small GTPases in *Entamoeba*: annotation of *E. invadens* Rab and its use for the understanding of *Entamoeba* biology. *Exp Parasitol* **126:** 337–347.

Nakada-Tsukui, K., Tsuboi, K., Furukawa, A., Yamada, Y., and Nozaki, T. (2012) A novel class of cysteine protease receptors that mediate lysosomal transport. *Cell Microbiol* **14:** 1299–1317.

Nakatogawa, H., Ichimura, Y., and Ohsumi, Y. (2007) Atg8, a ubiquitin-like protein required for autophagosome formation, mediates membrane tethering and hemifusion. *Cell* **130:** 165–178.

Nakatogawa, H., Suzuki, K., Kamada, Y., and Ohsumi, Y. (2009) Dynamics and diversity in autophagy mechanisms: lessons from yeast. *Nat Rev Mol Cell Biol* **10:** 458–467.

Nilsson, J.R. (1984) On starvation-induced autophagy in *Tetrahymena*. *Carlsberg Res Commun* **49:** 323–340.

Nozaki, T., Asai, T., Sanchez, L.B., Kobayashi, S., Nakazawa, M., and Takeuchi, T. (1999) Characterization of the gene encoding serine acetyltransferase, a regulated enzyme of cysteine biosynthesis from the protist parasites *Entamoeba histolytica* and *Entamoeba dispar*. Regulation and possible function of the cysteine biosynthetic pathway in *Entamoeba*. *J Biol Chem* **274:** 32445–32452.

Nozaki, T., Kobayashi, S., Takeuchi, T., and Haghighi, A. (2006) Diversity of clinical isolates of *Entamoeba histolytica* in Japan. *Arch Med Res* **37:** 277–279.

Okada, M., Huston, C.D., Mann, B.J., Petri, W.A., Jr, Kita, K., and Nozaki, T. (2005) Proteomic analysis of phagocytosis in the enteric protozoan parasite *Entamoeba histolytica*. *Eukaryot Cell* **4:** 827–831.

Okada, M., Huston, C.D., Oue, M., Mann, B.J., Petri, W.A., Jr, Kita, K., and Nozaki, T. (2006) Kinetics and strain variation of phagosome proteins of *Entamoeba histolytica* by proteomic analysis. *Mol Biochem Parasitol* **145:** 171–183.

Otto, G.P., Wu, M.Y., Kazgan, N., Anderson, O.R., and Kessin, R.H. (2003) Macroautophagy is required for multicellular development of the social amoeba *Dictyostelium discoideum*. *J Biol Chem* **278:** 17636–17645.

Paz, Y., Elazar, Z., and Fass, D. (2000) Structure of GATE-16, membrane transport modulator and mammalian ortholog of autophagocytosis factor Aut7p. *J Biol Chem* **275:** 25445–25450.

Picazarri, K., Nakada-Tsukui, K., and Nozaki, T. (2008a) Autophagy during proliferation and encystation in the protozoan parasite *Entamoeba invadens*. *Infect Immun* **76:** 278–288.

Picazarri, K., Nakada-Tsukui, K., Sato, D., and Nozaki, T. (2008b) Analysis of autophagy in the enteric protozoan parasite *Entamoeba*. *Methods Enzymol* **451:** 359–371.

Popovic, D., Akutsu, M., Novak, I., Harper, J.W., Behrends, C., and Dikic, I. (2012) Rab GTPase-activating proteins in autophagy: regulation of endocytic and autophagy pathways by direct binding to human ATG8 modifiers. *Mol Cell Biol* **32:** 1733–1744.

Saftig, P., and Klumperman, J. (2009) Lysosome biogenesis and lysosomal membrane proteins: trafficking meets function. *Nat Rev Mol Cell Biol* **10:** 623–635.

Saito-Nakano, Y., Yasuda, T., Nakada-Tsukui, K., Leippe, M., and Nozaki, T. (2004) Rab5-associated vacuoles play a unique role in phagocytosis of the enteric protozoan parasite *Entamoeba histolytica*. *J Biol Chem* **279:** 49497–49507.

Saito-Nakano, Y., Loftus, B.J., Hall, N., and Nozaki, T. (2005) The diversity of Rab GTPases in *Entamoeba histolytica*. *Exp Parasitol* **110:** 244–252.

Saito-Nakano, Y., Mitra, B.N., Nakada-Tsukui, K., Sato, D., and Nozaki, T. (2007) Two Rab7 isotypes, EhRab7A and EhRab7B, play distinct roles in biogenesis of lysosomes and phagosomes in the enteric protozoan parasite *Entamoeba histolytica*. *Cell Microbiol* **9:** 1796–1808.

Sambrook, J.A.R., and Russell, D.W. (2001) *Molecular Cloning*. Cold Spring Harbor, NY: Cold Spring Harbor Laboratory Press.

Sanchez, L., Enea, V., and Eichinger, D. (1994) Identification of a developmentally regulated transcript expressed during encystation of *Entamoeba invadens*. *Mol Biochem Parasitol* **67:** 125–135.

Somlata, Bhattacharya, S., and Bhattacharya, A. (2011) A C2 domain protein kinase initiates phagocytosis in the protozoan parasite *Entamoeba histolytica*. *Nat Commun* **2:** 230.

Sugawara, K., Suzuki, N.N., Fujioka, Y., Mizushima, N., Ohsumi, Y., and Inagaki, F. (2004) The crystal structure of microtubule-associated protein light chain 3, a mammalian homologue of *Saccharomyces cerevisiae* Atg8. *Genes Cells* **9:** 611–618.

Takeshige, K., Baba, M., Tsuboi, S., Noda, T., and Ohsumi, Y. (1992) Autophagy in yeast demonstrated with proteinase-deficient mutants and conditions for its induction. *J Cell Biol* **119:** 301–311.

Tillack, M., Nowak, N., Lotter, H., Bracha, R., Mirelman, D., Tannich, E., and Bruchhaus, I. (2006) Increased expression of the major cysteine proteinases by stable episomal transfection underlines the important role of EhCP5 for the pathogenicity of *Entamoeba histolytica*. *Mol Biochem Parasitol* **149:** 58–64.

Tomlins, A.M., Ben-Rached, F., Williams, R.A., Proto, W.R., Coppens, I., Ruch, U., *et al*. (2013) *Plasmodium falciparum* ATG8 implicated in both autophagy and apicoplast formation. *Autophagy* **9:** 1540–1552.

Tsukada, M., and Ohsumi, Y. (1993) Isolation and characterization of autophagy-defective mutants of *Saccharomyces cerevisiae*. *FEBS Lett* **333:** 169–174.

Wang, R.C., and Levine, B. (2010) Autophagy in cellular growth control. *FEBS Lett* **584:** 1417–1426.
Weidberg, H., Shpilka, T., Shvets, E., Abada, A., Shimron, F., and Elazar, Z. (2011) LC3 and GATE-16 N termini mediate membrane fusion processes required for autophagosome biogenesis. *Dev Cell* **20:** 444–454.
WHO (1997) WHO/PAHO/UNESCO report. A consultation with experts on amoebiasis. Mexico City, Mexico 28–29 January, 1997. *Epidemiol Bull* **18:** 13–14.
Williams, R.A., Woods, K.L., Juliano, L., Mottram, J.C., and Coombs, G.H. (2009) Characterization of unusual families of ATG8-like proteins and ATG12 in the protozoan parasite *Leishmania major*. *Autophagy* **5:** 159–172.

Supporting information

Additional Supporting Information may be found in the online version of this article at the publisher's web-site:

Fig. S1. Alignment of Atg8 in *Entamoeba* and other organisms. (A) Atg8 protein sequences from *Entamoeba histolytica* (a, XP_649165; b, XP_649940), *Entamoeba dispar* (1, XP_001736059; 2, XP_001735824), *Entamoeba moshkovskii* (1, EMO_027800; 2, EMO_113660; 3, EMO_031640) (Amoeba DB, http://amoebadb.org/amoeba/), *Entamoeba nuttalli* (1-378bp of scaffold JH928776 in Amoeba DB) and *Entamoeba invadens* (XP_004257811) were aligned by ClustalW. (B) Atg8 and its homologues from *Saccharomyces cerevisiae* (NP_00947), *Dictyostelium discoideum* (EAL64271), *Homo sapiens* (NP_009209), *Tetrahymena thermophila* (EAR86305) and *Trypanosoma brucei* (A, XP_846213; B, XP_846214) were aligned with *E. histolytica* Atg8a and Atg8b. NHD and ULD are indicated by dashed and solid lines respectively. A dot indicates an amino acid replacement in EhAtg8b.

Fig. S2. Detection of *EhAtg8a* and *EhAtg8b* transcripts by RT-PCR. (A) Schematic diagram of the two *Atg8* genes in *Entamoeba histolytica*. *EhAtg8b* contains a unique VspI site. (B) *EhAtg8a* and *EhAtg8b* transcripts were amplified by PCR using isotype-specific oligonucleotide primers and cDNA synthesized with (cDNA) or without (-RT) reverse transcriptase. (C) Verification of the identity of the *EhAtg8a* and *EhAtg8b* transcripts. *EhAtg8a* and *EhAtg8b* transcripts were amplified by RT-PCR and digested with (+VspI) or without VspI (–VspI).

Fig. S3. Ubiquitous expression of Atg8 in *Entamoeba histolytica* clinical isolates. Immunoblot analysis of EhAtg8 in clinical isolates. All strains were either monoxenically cultivated with *Crithidia fasciculata* or axenically cultivated, harvested at semi-confluence (2 or 3 days) and approximately 5 μg of the samples were analysed by SDS-PAGE and immunoblotting. The double arrows indicate the doublet bands of the membrane-associated form of EhAtg8.

Fig. S4. Additional immunofluorescent images of Atg8-associated phagosomes. Methods and conditions should be referred to the legend of Fig. 5A. Briefly, *Entamoeba histolytica* trophozoites of HM-1 strain were co-cultured with CellTracker Blue-loaded CHO cells for the indicated times, fixed and then reacted with anti-EhAtg8 antibody and Alexa-568 conjugated anti-rabbit IgG secondary antibody. Arrows indicate phagosomes with EhAtg8. Two additional cells are shown for each time point.

Fig. S5. Additional immunofluorescent images showing the association of Atg8 with the phagocytic cup. Methods and conditions should be referred to the legend of Fig. 6. Briefly, *Entamoeba histolytica* trophozoites of pSAP2 control transformant (with G3 background) were co-cultured with CellTracker Blue-loaded CHO cells for 10 min (upper panels) or 30 min (lower panels), fixed and then reacted with anti-EhAtg8 and anti-EhVps26 antibodies labelled with Alexa Fluor 488 or Alexa Fluor 546 by ZENON rabbit IgG labeling kit.